

Article

Not peer-reviewed version

Does Regulated Deficit Irrigation Affect Pear Fruit Texture by Modifying the Stone Cells?

[Jesús D. Peco](#) , [Hava F Rapoport](#) , [Ana Centeno](#) ^{*} , [David Pérez-López](#) ^{*}

Posted Date: 25 September 2023

doi: 10.20944/preprints202309.1640.v1

Keywords: *Pyrus communis*; pear; regulated deficit irrigation; stone cells; fruit quality



Preprints.org is a free multidiscipline platform providing preprint service that is dedicated to making early versions of research outputs permanently available and citable. Preprints posted at Preprints.org appear in Web of Science, Crossref, Google Scholar, Scilit, Europe PMC.

Copyright: This is an open access article distributed under the Creative Commons Attribution License which permits unrestricted use, distribution, and reproduction in any medium, provided the original work is properly cited.

Article

Does Regulated Deficit Irrigation Affect Pear Fruit Texture by Modifying the Stone Cells?

Jesús D. Peco^{1,3}, Hava F. Rapoport², Ana Centeno^{3,*} and David Pérez-López^{3,*}

¹ Dpto. Producción Vegetal, ETSIA–Universidad de Castilla–La Mancha, Ronda de Calatrava, 13003 Ciudad Real, Spain.

² Instituto de Agricultura Sostenible (IAS), Consejo Superior de Investigaciones Científicas (CSIC), Avenida Menéndez Pidal s/n, Córdoba, Spain.

³ Dpto. Producción Agraria, CEIGRAM-Universidad Politécnica de Madrid, Av. Puerta de Hierro, 2, 28040 Madrid, Spain.

*Correspondence: ana.centeno@upm.es; david.perezl@upm.es

Abstract: Regulated deficit irrigation (RDI) strategies aim to improve water usage without reducing yield. Generally, irrigation strategy effectiveness is measured as fruit yield, with little consideration of fruit quality. As water deficit and increased plant cell sclerification often associated, this study explores the effect of RDI on pear fruit stone cells, a crucial factor affecting flesh texture. The presence, distribution and development of pear fruit stone cells under RDI and full irrigation are compared using *Pyrus communis* L. cv. Barlett trees, employing recently developed microscope image analysis technology. The Control treatment was maintained under non-stress conditions, while the RDI treatment received an average of 15% of Control water during the latter part of Stage I fruit development. Observations at the end of Stage I and at harvest showed no effect on stone cell presence under the tested RDI strategy. Relative area of stone cells within the flesh was greater at Stage I than at harvest, as stone cell expansion occurred early in development while the (unsclerified) parenchyma cells, dominant component of the fruit flesh, expanded until harvest. Stone cell cluster density was higher near the fruit core than in the cortex center and exterior. These initial results suggest that well-planned RDI strategies will generally not affect pear fruit stone cell content and thus, textural quality. Microscope image analysis supported results from previously used analytical techniques, principally chemical, while providing a tool for better understanding the process and timing of stone cell differentiation and thus testing the factors involved.

Keywords: *Pyrus communis*; pear; regulated deficit irrigation; stone cells; fruit quality

1. Introduction

Water availability is essential for profitable production of many woody fruit crops, although with water resources often scarce or costly, requiring improved water use efficiency [1]. Regulated Deficit Irrigation (RDI) strategies were proposed as a solution to this challenge. This approach takes advantage of the varied sensitivity to water stress at different times during fruit growth to minimize the impact of reduced irrigation on yield [2,3].

RDI strategies have been reported as a successful method for pear cultivation without reducing yield by Mitchel et al. [4] and Vélez-Sánchez et al. [5], for European pear (*Pyrus communis*) and Caspari et al. [6], Behboudian et al. [7] and Wu et al. [8,9] for Asian pear (*P. serotina* and *P. bretschneideri*), among others. The deficit period is carried out at a time when fruit growth is least reduced, and if so, can later recuperate sufficiently so that yield reduction is small. Pear fruit growth is driven by the cell division and expansion of the fruit flesh, and consists of two periods. In Stage I the main proportion of cell division takes place, along with some cell expansion which is masked by concurrent cell division, and in Stage II only cell expansion occurs [10]. Marsal et al. [11], for example, applied RDI strategies during latter part of pear fruit development Stage I, finding only a slight

tendency for RDI fruits to be smaller. The successful application of the water deficit during Stage I rather than Stage II concurs with the classical analysis by Hsiao [12], suggesting that highly active cell expansion during Stage II generates greater water-stress sensitivity in that period than in Stage I.

In establishing the RDI strategy, however, as in many other fruit crops, successful management of the pear crop is basically evaluated as yield in size and/or weight, but little attention has been paid to fruit quality. In establishing the RDI strategy, however, as in many other fruit crops, success is basically evaluated as yield in size and/or weight but little attention has been paid to fruit quality. Preliminary results under tropical conditions seem to indicate that RDI strategies did not affect the fruit firmness, pigments, color index, or content of phenols, sugar or acids [5]. However stone cell content, a crucial factor contributing to pear fruit quality by negatively effecting texture, has yet to be examined under RDI application.

While the pear fruit flesh is principally composed of parenchyma cells, many stone cells or sclereids are also present. For example, in fruits of *P. communis* at the end of Stage I, up to 35% of the pulp cell number may be stone cells [10]. These cells, a type of relatively isodiametric sclereid known as brachysclereid, are formed by the deposition of a lignified secondary wall within the primary walls of parenchyma cells [13] and are present either isolated or in aggregated groups referred to as stone cell clusters (SCCs) [14,15]. The presence of high concentrations of stone cells increases the roughness of the flesh texture, reducing economic value [16]. Stone cell formation starts 7–15 days after full bloom (DAFB), and their further development, consisting of additional lignified thickening of the cell wall, continues until approximately 50–65 DAFB, when they reach their maximum size in most varieties [15,17]. Several factors influence the formation of SCCs, including climate, agricultural practices and post-harvest handling, however, the tree variety is considered to be the most important [18–21].

Plant water deficit has been frequently associated with increased cellular lignification [22]. Studies of pear trees suggest that water stress during the early stages of fruit growth increases the stone cell content in pear flesh, associated with the activity of peroxidase enzyme (POD), to produce greater cell wall lignification [23]. However this observed effect is not well known and seems to depend on the tree variety and its resistance, as well as the intensity, duration and the period in which water stress is suffered [16]. Furthermore, it is important to consider how the different cellular processes (cell division, cell enlargement, and differentiation) might be involved in response to water stress. That is, once a stone cell initiates formation from a parenchyma cell, the onset of the secondary cell wall lignification prevents further cell expansion, although cell differentiation continues as lignification progresses towards the interior of the cell [10,16]. Thus water deficit might act by stimulating the initiation of more stone cells or by increasing lignification of the already initiated cells. Lee et al. [18], basing their observations on fresh- and dry-weight measurements, suggested that water deficit increased lignin deposition.

The main goal of this study was to elucidate the effects that RDI strategies might have on the pear flesh quality, in particular on the stone cell content. Newly developed microscope image analysis technology was employed to quantify cellular properties such as size, development and distribution of stone cells within the parenchyma cell matrix, providing essential information for understanding and testing the factors involved in stone cell formation.

2. Materials and Methods

2.1. Growth conditions

Two-year-old pear trees *Pyrus communis* var Williams were planted in 120 L containers. During the first year of growth in the containers (year three), the limits of plant water stress for local conditions were established using stem water potential (Ψ_{stem}) and photosynthetic parameters measured with pressure chamber and IRGA system. In the following two years after planting, two irrigation regimes, Control and Regulated Deficit Irrigation (RDI) were tested in the now four- and five-year-old trees. For the control treatment, irrigation was carried out to provide non-stress conditions in the plants, maintaining the average Ψ_{stem} above -0.8 MPa. RDI plants were exposed to

a deficit irrigation period within the latter part of fruit growth Stage I (32–60 DAFB), in which the applied water was gradually reduced until the values of Ψ_{stem} reached around -1.4 MPa. More details about crop growth conditions are described by Marsal et al. [11].

2.2. Fruit tissue sampling and preparation

In the second year of the RDI experiment fruits were collected at the end of Stage I and at harvest (end of Stage II). A 5 mm transverse slice at the widest portion of the fruit was taken from 12 (Control) and 14 (RDI) fruits per treatment, using 2–4 fruits per tree on four trees per treatment at the end of Stage I and the same number of fruits per tree on two trees per treatment at final harvest (Stage II). The slices were fixed in FAE (formalin: acetic acid: 60% ethanol, 2:1:17, v/v/v) and preserved in 70% ethanol. Standardized portions of the fruit cortex were identified by first staining the complete slices for 2–3 h in 70% ethanol with weak toluidine blue [24] to show the different vascular bundles (associated with sepals, petals, and carpels) present in pome fruit. Three wedge-shaped radial sectors extending from the sepal vascular bundle (SB) to the fruit exterior were cut per fruit slice (Figure 1). The sectors were dehydrated in tertiary butyl alcohol and processed according to standard paraffin procedures, obtaining microtome sections of 10–12 μm , which were stained with tannic acid, iron chloride, safranin and fast green, adapted from Johansen [25] and Ruzin [26].

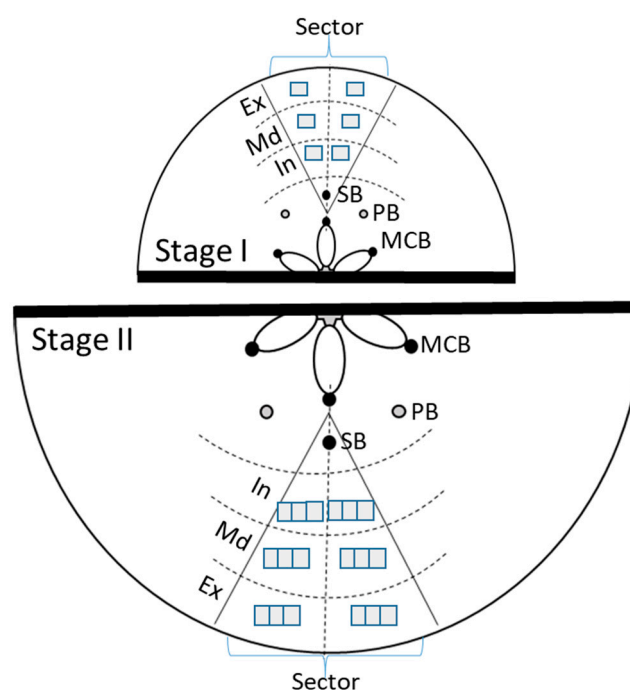


Figure 1. Scheme for analysis of pear fruit cells in sections of Stages I (upper) and II (lower). For each stage, 3 wedge-shaped sectors were cut from each transverse fruit slice, each extending from a sepal bundle (SB) to the fruit exterior, and processed for histological study. For measurements, the sector was visually divided into two halves, and three concentrically oriented zones Ex (Exterior), Md (Middle) and In (Interior). The squares within each zone represent the number of microscope image areas (0.06 cm^2) captured and analyzed (two images per zone for Stage I, six per zone for Stage II). SB: sepal bundle, PB: petal bundle, MCB: median carpelary bundle.

2.3. Histological assessment

For histological evaluation the fruit sectors were divided at equal distances along the radius into three concentrically oriented zones: the area closest to the fruit Exterior (zone Ex), the intermediate or Middle zone (zone Md), and the area closest to the fruit Interior (Zone In) as depicted in Figure 1. Two square images per zone, each 0.06 cm^2 , were observed in each histological section for Stage I, and six images per zone for Stage II. Microscopic images were acquired with an Olympus BX51 light

microscope and recorded by a digital camera (Olympus SC50) attached to the microscope using Cell Sense Imaging Software (Olympus). All parameters were first determined for the three different fruit-flesh zones, and then overall (globally) for the total area studied. The global values were calculated by considering the proportional area contribution of each zone.

Individual stone cells and stone-cell clusters were observed. Stone-cell clusters, referred to as SCCs following the nomenclature of Nii et al. [14], were considered as such when the cluster contained more than three adjoining stone cells. Individual stone cells and those found in groups of two or three, in all cases separated from other stone cells by at least one parenchyma cell, were designated as isolated. Given the relatively small number of isolated stone cells (Figure 2D), the majority of the stone cell analyses utilized only the SCC's. A macro was developed for use with Image J software (V.2.1.0) to automatically determine the size of the SCCs, the number of SCCs and isolated stone cells, the area occupied by the SCCs, and the number of SCCs per area. In addition, average stone cell size was calculated from the data.

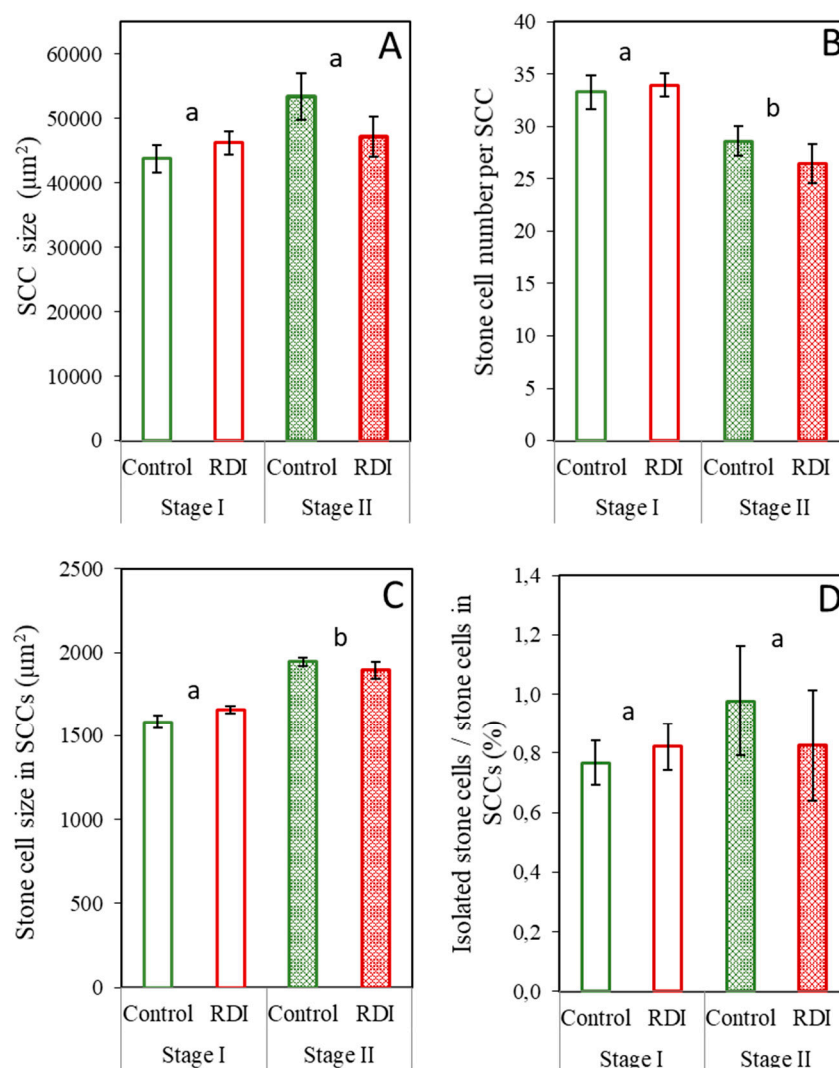


Figure 2. SCC attributes across the complete fruit flesh area: SCC size (A), stone cell number per SCC (B), stone cell size in SCCs (C) percentage of isolated stone cells compared to the stone cells within SCCs (D). Treatments were two irrigation regimes (control and Regulated Deficit Irrigation, RDI) sampled at two different times (Stage I and II). Error bars represent the standard error. No significant differences were found at $P \leq 0.05$ between treatments (t-student's test). Values with different lowercase letters are significantly different between stages at $P \leq 0.05$ (t-student's test).

The parenchyma cells were divided into two types: those with and without direct contact with stone cells, and a second Image J software (V.2.1.0) macro was established for measuring parenchyma cell size and circularity index. The internal size of each cell was identified, measured, and average cell size calculated. A circularity shape index ranging from 0 to 1 was used to assess the roundness of the cells, in which values closer to 1 indicate more circular shape and closer to 0 a more elliptical shape. To obtain this value, the largest and smallest diameters of each parenchyma cell were automatically measured, and the following equation was used:

$$\text{Mesocarp cell circularity} = \text{Largest diameter} / \text{Smallest diameter}$$

2.4. Fruit tissue sampling and preparation

All the data reported were tested for homogeneity of variance and normal distribution, and then analyzed using analysis of variance (ANOVA) followed by Tukey test, or Student's t-test to determine the significant differences ($p \leq 0.05$). In two analyses which considered percentages, that is, 1) the percentage area occupied by SCCs and 2) the ratio of isolated stone cell number to the numbers of stone cells in SCCs, were subjected to arcsine transformation before ANOVA. Statistical analysis was performed by SPSS V24.0.

3. Results

3.1. Stone cells under RDI and control irrigation

Characteristics of the SCCs present in the fruit flesh did not differ between the RDI and control treatments (Figure 2). That is, SCC size, SCC cell number, and SCC cell size showed no significant differences between irrigation treatments at either sampling times. Between sample times SCC size remained the same (Figure 2A), while stone cell number per SCCs decreased and, in parallel, mean stone cell size in SCCs increased (Figure 2B, C). The percentage of isolated stone cells (found in groups of 3 or less) was quite small when contrasted with SCCs (Figure 2D), and, although slightly more variable than the other SCC parameters presented in Figure 2, was statistically similar between treatments and sample times.

The SCC presence in the fruit transverse section, observed as the percentage of tissue area occupied by SCCs and as number of SCCs per cm^2 , was the same for the control and RDI treatments at each analyzed time (Figure 3). Although no significant differences were found between irrigation treatments, however, there was a dramatic decrease in both of those parameters between Stage I and Stage II.

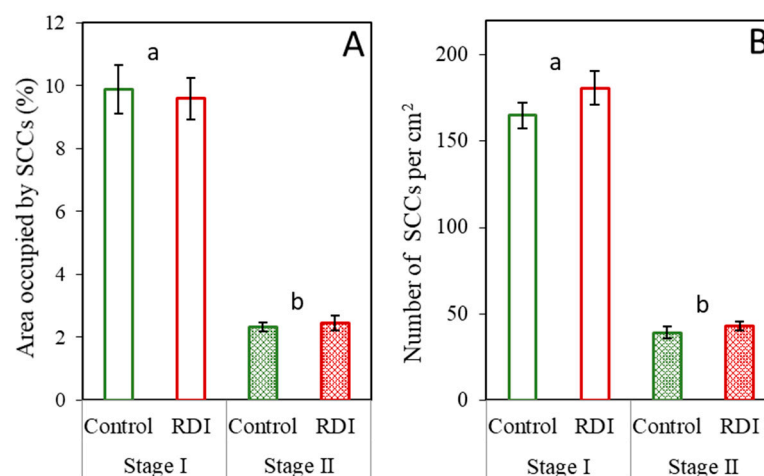


Figure 3. Presence of SCCs in fruit transverse sections determined as percentage of area occupied (A) and number of SCCs per cm^2 (B). Observations of pear fruit under two irrigation regimes (control and Regulated Deficit Irrigation, RDI) at two different times (Stage I and II). The error bars represent the

standard error. No significant differences were found at $P \leq 0.05$ between treatments (t-student's test). Values with different lowercase letters are significantly different between stages at $P \leq 0.05$ (t-student's test).

Similarly to the whole flesh analysis (Figures 2 and 3), when the different zones within the fruit flesh were analyzed separately, no significant differences in SCC characteristics (Figure 4) or presence (Figure 5) were observed between control and RDI treatments within each zone at either time. For some of the parameters studied, however, some differences were observed among zones or between sample times, in spite of the consistent values between treatments.

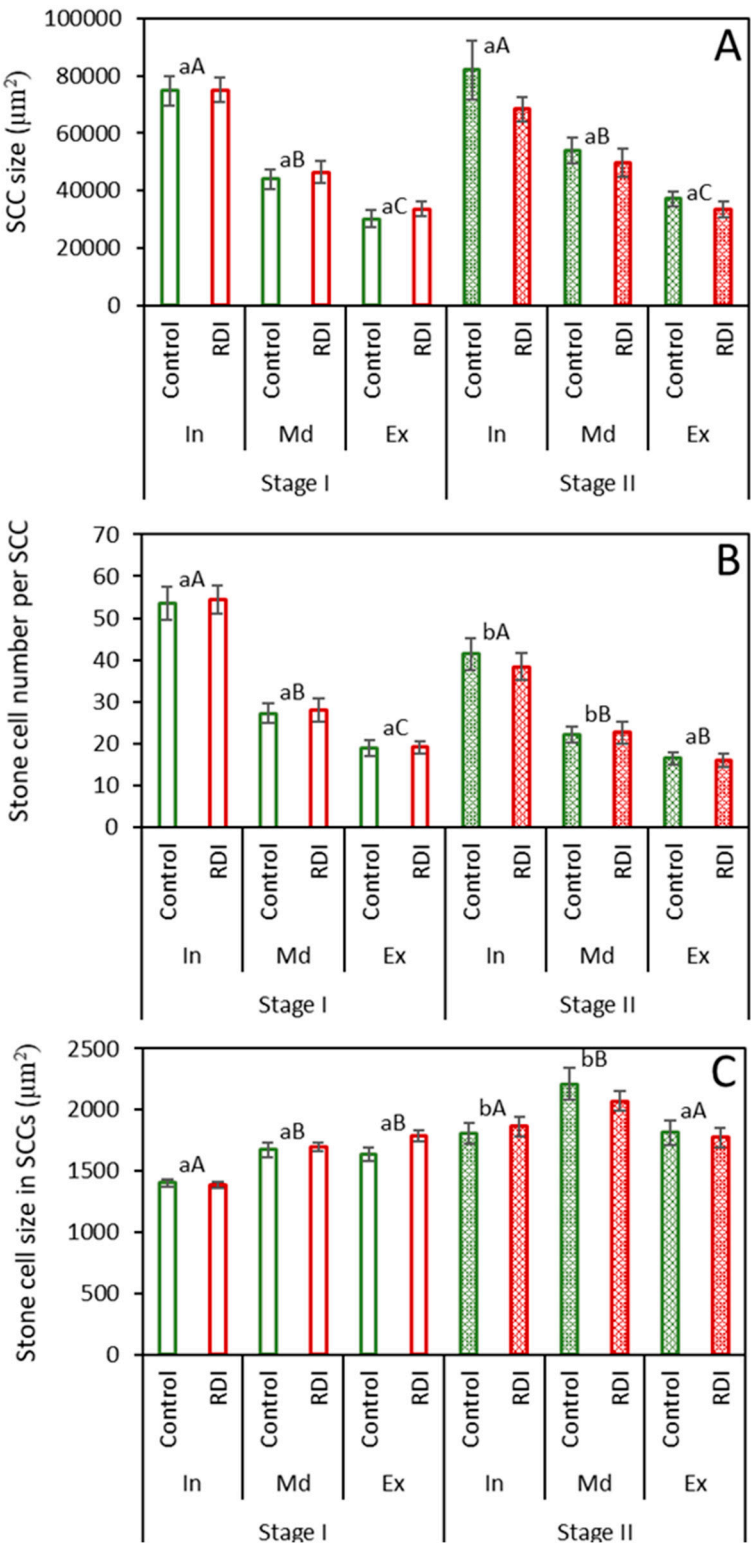


Figure 4. SCC and SCC cell attributes in separate concentric zones in transverse slices of pear: SCC size (A), stone cell number per SCC (B) and stone cell size in SCCs (C) under two irrigation regimes (control and Regulated Deficit Irrigation, RDI) at two times (Stage I and II). Zone In is closest to the fruit center, Zone Md intermediate, and Zone Ex closest to the exterior. Error bars represent standard error. No significant differences were found at $P \leq 0.05$ between treatments (t-student's test). Values with different lowercase letters were significantly different between stages, and values with different capital letters were significantly different between zones at $P \leq 0.05$ (t-student's test and ANOVA, Tukey test).

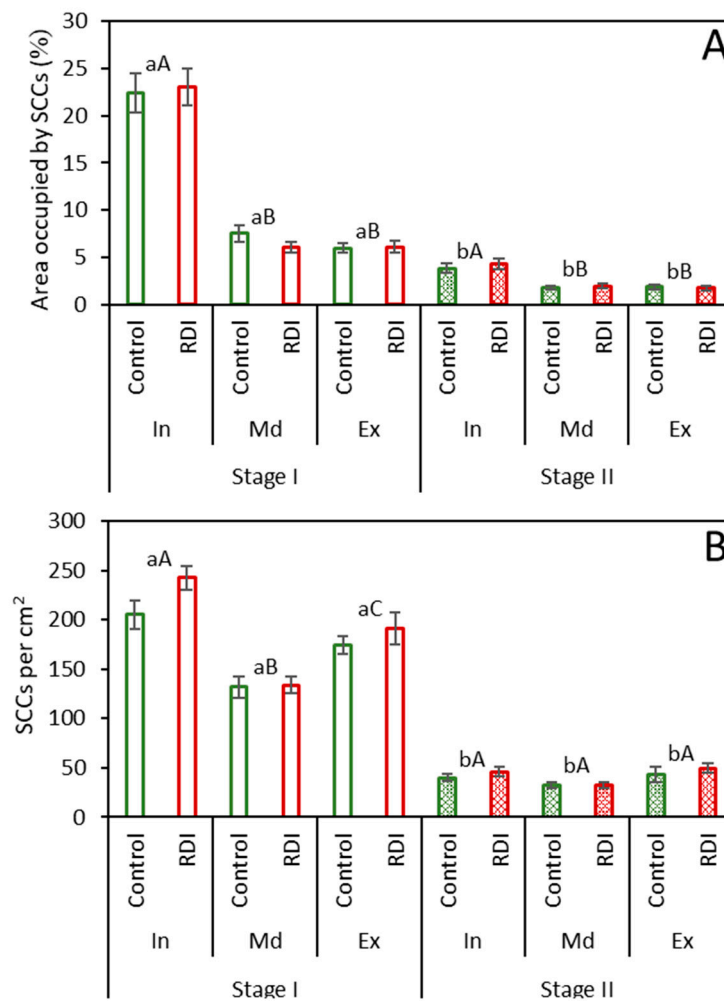


Figure 5. Presence of SCCs in concentric zones of pear fruit transverse sections. Data presented as percentage of area occupied by SCCs (A) and number of SCCs per area (B) under two irrigation regimes (control and Regulated Deficit Irrigation, RDI) at two different times (Stage I and II). Zone In (Interior) nearest the fruit center, Zone Md (Middle), and Zone Ex (Exterior) closest to the fruit exterior. Error bars represent the standard error. No significant differences were found at $P \leq 0.05$ between treatments (t-student's test). Values with different lowercase letters were significantly different between stages, and values with different capital letters were significantly different between zones at $P \leq 0.05$ (t-student's test and ANOVA, Tukey test).

3.2. Stone cell dimensions and presence in different fruit zones

When comparing concentric zones within the fruit, SCC size presented a significant pattern of successive decrease from zone In (closest to fruit interior) to zone Ex (closest to fruit exterior), but neither that pattern nor the specific values obtained in each zone varied between stages (Figure 4A). The number of sclereids per SCC (Figure 4B) also showed a similar pattern of successive decrease

among zones, although there were some differences between stages. For one, cell number per SCC in zones In and Md decreased between Stage I and II. In addition, while SCC cell number was significantly different among all three zones at Stage I, there was no significant difference between zones Md and Ex at Stage II for that parameter. Stone cell size presented lesser differences than SCC size and cell number, but some clear-cut differences among zones (Figure 4C). Zone In cells were the smallest at both stages, zone Md cells larger, and zone Ex (most exterior) cells similar to those of zone Md at Stage I and zone In at Stage II. Between stages, an increase in cell size was observed for zones In and Md, but not zone Ex.

Among zones, when the presence of SCCs was measured as, percent area, its extent was considerably higher for zone In at Stage I than for the other zones at the same stage and all zones at Stage II (Figure 5A). In contrast, when SSC presence was viewed as number per cm², values for all three zones were relatively high at Stage I, although significantly greatest for zone In, lowest for zone Md, and intermediate for zone Ex (Figure 5B). Between fruit development Stages I and II there was a significant decrease in stone cell presence in all zones, although with different magnitude according to parameter and zone (Figure 5A,B). Thus, percent area occupied by SCCs was highly reduced in zone In, with a less marked decrease in zones Md and Ex (Figure 5A). When presence was viewed as number of SCCs per cm², however, the reduction from Stage I to II was more comparable among zones (Figure 5B).

3.3. Cellular differentiation in the fruit flesh

Differentiation of the SCCs is shown in Figure 6. At Stage I (Figure 6A,B) the stone cells in many of the clusters presented mixed degrees of sclerification, as observed by the different degrees of lignified wall thickening (observed as red with the histological stain utilized in this study). That is, some of the cells forming stone cells or sclereids, presented early stages observed with a thin ring of only slightly lignified walls and most of the cell's cytoplasm still present. Other cells showed successively greater cell wall thickening and a decrease in cytoplasm, ultimately producing a highly thickened cell wall which fills the entire cell. Notably, the cells positioned farther away from the SCC center showed lesser degrees of lignification compared to the central cells. Complete SCC differentiation, observed principally in Stage II, was indicated by full lignification observed in all the stone cells of the cluster (Figure 6C,D).

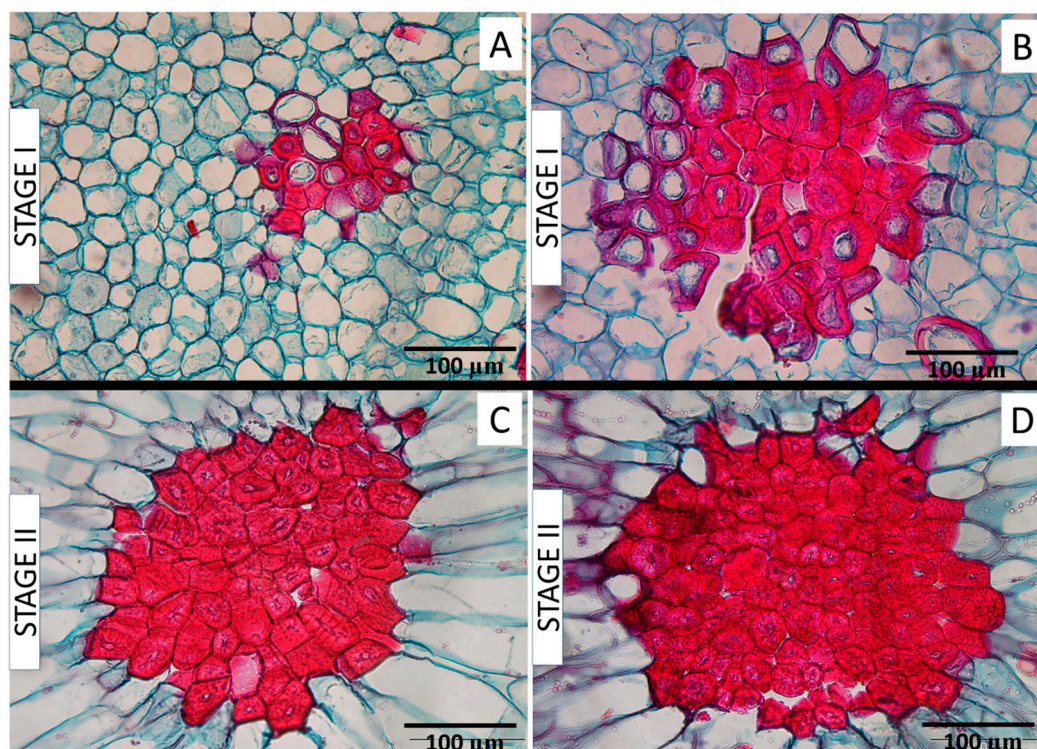


Figure 6. SSCs in transverse sections of the cortical flesh of pear fruit presenting varied degrees of differentiation of the clusters and their component cells. Mixed degrees of cell wall sclerification (lignification; red stain) observed in Stage I (A, B) and complete sclerification of all cluster cells in Stage II (C, D).

At Stage II, in addition to being composed of fully differentiated stone cells, some clusters were observed in which parenchyma cells were present within the clusters, seemingly breaking them into multiple groupings (Figure 7A,B). Most of the clusters, however, were exclusively composed of stone cells as in Figure 6C,D.

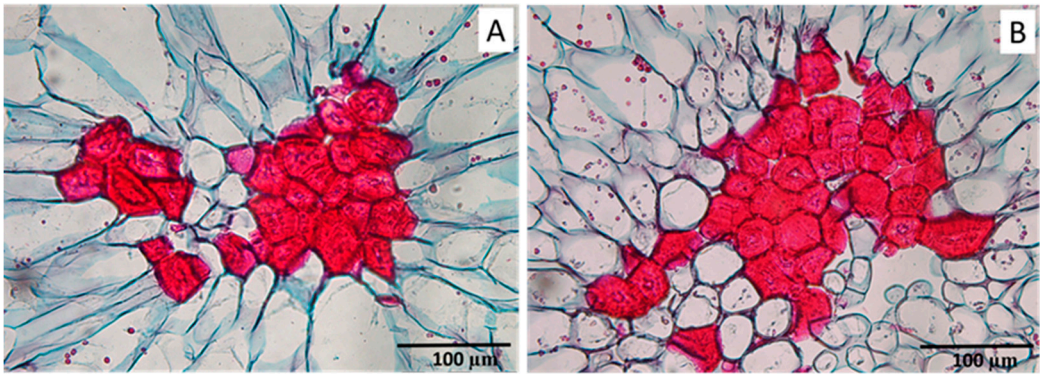


Figure 7. Stone cell clusters in which there are stone cells separated from the main SCC by parenchyma cells. Observed in Stage II; images from the control treatment. Stone cells have thick red cell walls; parenchyma cells have thin dark or blue cell walls.

The sizes of the parenchyma cells with and without contact with SCCs were comparable between irrigation treatments (Table 1). Nonetheless, a minor though non-significant tendency was observed for the RDI parenchyma cells to be approximately 10% smaller than those of the control in both Stage I and Stage II (Table 1). Parenchyma cell shape was not influenced by the RDI regime (Table 2).

Table 1. Parenchyma cell sizes in pear fruit flesh at stage I and II for two irrigation treatments (control and Regulated Deficit Irrigation, RDI). The transverse sections were measured in three concentric zones (In, Interior; Md, Middle; Ex, Exterior), and the parenchyma cells were divided into general (all parenchyma cells except those in contact with stone cells) and around cluster (those in direct contact with the stone cells). Values show the means. No significant differences were found at $P \leq 0.05$ between treatments (t-student’s test). Values with different lowercase letters were significantly different between stages, and values with different capital letters were significantly different between type of parenchyma cell $P \leq 0.05$ (t-student’s test and ANOVA, Tukey test).

		Size (μm ²)	
		Parenchyma cells (general)	Parenchyma cells around cluster
Stage I	Control	In	2147aA
		Md	3034aA
		Ex	3154aA
	RDI	In	1879aA
		Md	2956aA
		Ex	2889aA
Stage II	Control	In	9472bA
		Md	13435bA
		Ex	13139bA
	RDI	In	8706bA
		Md	13400bA
			7276bA

Ex11327bA9658bB

A considerable, approximately 3-fold increase in parenchyma cell size was observed from Stage I to Stage II for parenchyma cells both without and with contact with SCCs (Table 1). That size increment was even greater in zones A and B than in Zone C, and comparable rises were noted in the parenchyma cells around the clusters. With respect to contact with the clusters it was found that parenchyma cells around the SCCs were substantially smaller than parenchyma cells in all fruit zones and at both stages.

Parenchyma cell shape changed between Stage I and II, becoming less circular (Table 2). That is, Stage I cells were found to be rounder, whereas in Stage II they were more ellipsoidal. This can also be observed in Figure 8 cross-section images of pear flesh, in which Stage I parenchyma cells surrounding the cluster are more rounded (Figure 8A) compared to the more ellipsoidal cells in Stage II (Figure 8B). In comparing the parenchyma cells surrounding the clusters with those in the overall fruit flesh, no difference was found at Stage I, but in Stage II the cluster-surrounding cells were found to be more ellipsoidal than those in the rest of the fruit tissue (Table 2, Figure 8B). No differences were observed among zones in cell shape (data not shown).

Table 2. Parenchyma cell shape in pear fruit flesh, using a circularity index on a scale of 0 to 1. A value closer to 1 indicates a more circular shape (further details in Material and Methods). Data from stage I and II for two irrigation treatments (control and Regulated Deficit Irrigation, RDI). The parenchyma cells were divided into general (all parenchyma cells except those in contact with stone cells) and those in direct contact with the stone cells. Values show the means. No significant differences were found at $P\leq0.05$ between treatments (t-student’s test). Values with different lowercase letters were significantly different between stages, and values with different capital letters were significantly different between type of parenchyma cell $P\leq0.05$ (t-student’s test and ANOVA, Tukey test).

		Circularity (1-0)	
		Parenchyma cells (general)	Parenchyma cells around cluster
Stage I	Control	0.67 aA	0.67 aA
	RDI	0.62 aA	0.68 aA
Stage II	Control	0.58 bA	0.42 bB
	RDI	0.55 bA	0.45 bB

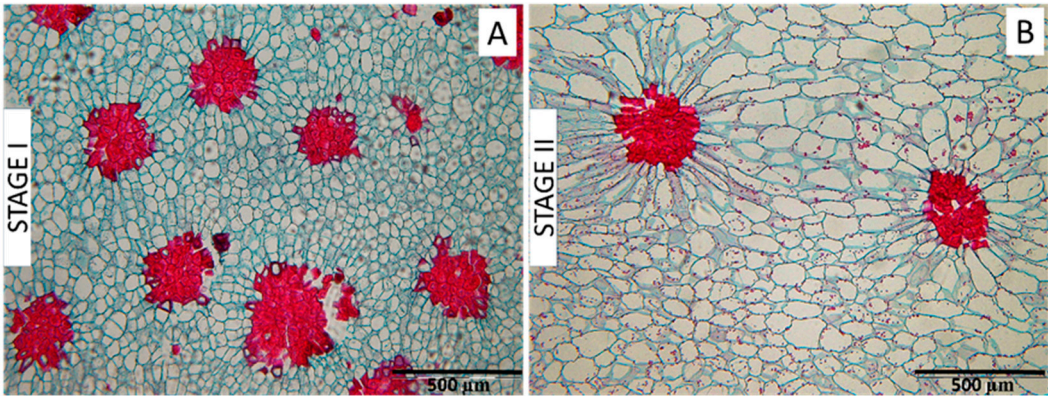


Figure 8. Variability in parenchyma cell shape based on fruit development and spatial relationship with SCCs. Images were obtained in control treatment of Stage I (A) and Stage II (B). Parenchyma cells are visualized with blue-stained cell walls, while SCCs are stained in red.

4. Discussion

4.1. Effect of RDI strategies on pear fruit stone cells

The RDI strategy examined in this study exhibited no discernible impact on the quantity and size of stone cells in pear fruit. Consequently it can be inferred that one of the fundamental goal of RDI strategies, to maintain fruit quality, has been successfully achieved. It is imperative to underscore that despite the presence of numerous studies in the literature that investigate the effects of RDI strategies on pear cultivation, these studies predominantly concentrate on quantifying water conservation, assessing tree growth, and analyzing fruit size [4–8,11]. There exists a gap, however, in evaluating the potential implications of these strategies on stone cell content, which substantially influences the textural attributes of the fruit. Hence this study demonstrates the applicability of these strategies in pear cultivation without worsening fruit texture.

In spite of earlier studies showing an increase in stone cell content as a result of water stress [18], we believe that, in our specific case, the application of stress after the critical phase of initial formation of sclereid primordial cells, along with the relatively mild intensity of the administered water, may have collectively contributed to the preservation of pear texture quality.

Sterling et al. [27] established that individual sclereids are initiated within the cortex of *Pyrus communis* cv. Barlett pears one - two weeks after bloom. Later, until 8 weeks after full bloom, the differentiation of new stone cells occurs principally in the parenchyma surrounding the previously formed sclereids, forming clusters. Consequently the quantity of SCCs is determined by the number of individual sclereids, formed during the very early stages of fruit growth [16]. The period of water stress we applied encompassed the interval from 32 to 60 DAFB, after the initial formation phase of sclereid cell initiation. That is, the early determination of individual stone cells would produce the similar SCC number we found between the control and RDI treatment, even though continued lignification and further stone cell differentiation would continue. As a result, we can affirm that in establishing RDI strategies, understanding the critical stages of fruit cell differentiation is crucial to prevent detrimental impacts on fruit quality.

Regarding the size of SCCs, experiments involving drought stress in *Pyrus pyrifolia* cv. niitaka demonstrated that intense water stress periods between 30 to 60 DAFB led to an increase in stone cells, quantified in terms of dry weight, in comparison to control fruits [22]. Those authors suggested that the increase in stone cells could be attributed to the decrease in leaf water potential, which hindered the absorption of calcium. As a result of this imbalance, there was an increase in peroxidase enzyme activity (POD) [22]. High POD activity is known for its role in promoting stone cell formation within the flesh, primarily due to the heightened cell wall lignification [23]. POD enzyme activity increases in response to stress factors, such as drought, producing augmented cell wall lignification [23,28]. This phenomenon can potentially be directly associated with the heightened stone cell presence in the pear fruit. However it is essential to consider that the water stress intensity in that experiment was considerably more severe than in our own, reaching leaf water potential values of – 2.7 MPa [22], whereas the lowest potential peak in our study was –1.7 MPa [11]. This implies that our plants might not have experienced a sufficiently pronounced stress level to trigger an elevation in POD enzyme activity and subsequently enhance the SCCs density per unit area. As a result, we agree that meticulous control of the water stress intensity applied to trees within RDI strategies is imperative to avoid high levels that could adversely impact fruit texture quality as advocated by Torrecillas et al. [29].

4.2. Stone cell and cluster development

Within the SSCs differences may be observed among the stone cells in their degree of differentiation, as shown in Figure 6. The pear fruit receptacle at bloom is composed of parenchyma cells, the majority of which will divide and expand during development to produce growth in fruit size, while some of them will differentiate into sclerified stone cells. In stone cell differentiation certain parenchyma cells develop a highly specialized secondary cell wall which thickens due to lignin deposition towards the interior of the cell, a process which continues progressively until the

entire cell walls are fully thickened [10,16,27]. In Stage I SCCs (Figure 6A,B) one can observe mature, fully lignified stone cells which are completely stained red for lignin, and others, less developed, in which the lignification is still in progress and appears as a ring. Cheng et al. [16] designated those partially lignified cells in which a lignified ring surrounds the shrinking cell lumen as sclereid primordia. Within the Stage I SCCs the fully mature sclereids are observed in the centers of the clusters, while the partially developed sclereid primordia are found towards the cluster exterior. These observations agree with interpretation by Sterling [27] that clusters are built as newer sclereids form around the earlier differentiated ones.

In the mature SCCs in Stage II (Figure 6C,D), the central stone cells in the cluster tend to be smaller than those more towards the cluster exterior. Once a stone cell begins to sclerify, its division and expansive growth stop due to the rigidity of secondary cell wall [30] and the degradation of vesicles and organelles present within these cells [14,19]. Since the growth of stone cells ceases upon the onset of lignification, the larger stone cells would seem to develop from larger parenchyma cells, present at a later moment in fruit expansion, further evidence of progressive formation of stone cells outwards from the cluster center [27]. Moreover, average stone cell size increased from Stage I to II (Figures 2C and 4C), also indicating the differentiation of sclereids from larger parenchyma cells formed later in fruit growth, as well as the occurrence of some lignification later than Stage I. This phenomenon was only evident, however, in the interior and middle zones of the flesh fruit. It is possible that stone cells situated more externally in the flesh fruit completed their formation earlier than those located deeper within the flesh fruit. However, this would contradict Esau et al. [30], who described that SCC formation begins in deeper regions of the pear flesh and progresses outward.

A slight reduction in the number of stone cells per SCC in Stage II compared to Stage I was found in the inner and middle zones (Figure 4B). This observation suggests that, in this pear variety, certain stone cells might become detached from the SCC, possible occurring by invasive parenchyma growth as can be observed in the microscopic images (Figure 7). This finding contradicts the previously postulated pattern of development, in which stone cell aggregation intensifies throughout the fruit develop [16]. Nonetheless, it is important to note that such instances of detachment were relatively uncommon, since the number of isolated stone cells encountered in the fruit pulp was significantly smaller compared to the number of stone cells grouped within SCCs. Also, this phenomenon was not uniformly observed throughout all parts of the flesh fruit but was limited to the inner and middle zones. The reduction in SCC size might hold significance due to the intrinsic connection between the texture of the fruit flesh and the size of SCCs [16]. In this manner, SCCs with diameters exceeding 250 μm yield a coarse and gritty flesh texture, those ranging between 150 μm and 250 μm offer a soft texture with a slight gritty sensation, and those less than 150 μm result in a highly soft texture [16,17]. Consequently, the separation of isolated stone cells from the SCC could possibly contribute to an improvement in the texture quality of the pear, but requires further research.

Limited information is available regarding the comprehensive characterization of SCCs within different regions of the fruit pulp, likely related to required time and available analytical techniques. Prior studies have convincingly demonstrated a higher overall quantity of SCCs in the inner fruit region across five pear cultivars [17,31], with only one variety showing a prevalence near the peel [17]. Our findings concur with these previous studies, indicating a substantial occurrence of SCCs in the inner zone, in contrast to the middle and exterior regions of the fruit. This observation could be attributed not only to an increased number of SCCs (in Stage I) but also to their larger size and a higher count of stone cells per SCC (in both Stage I and II). This pattern coincides with the findings of Tao et al. [31] and Li et al. [17], who reported that SCCs in the inner region were notably larger than those found in the remaining flesh.

4.3. Relationship of parenchyma development and SCCs

From Stage I to Stage II a substantial drop, to almost 20%, was found in the number and density (percent area) of SCCs (Figure 3). The decrease in relative presence of SSCs results from the interaction between stone cell differentiation and parenchyma cell expansive growth during fruit development. That is, on one hand, it has been shown in many studies and in a large number of

different varieties, that the pear fruit SCC content stabilizes around 50-65 DAFB [15,17,21], after which the stone cells remain static without growth and are not degraded after formation [14,16,32]. Secondly, cell expansion in parenchyma cells [11,17,19] continues throughout pear fruit growth, diluting the SCC density in the flesh fruit. In addition to the generally high SCC presence observed for the complete fruit at Stage I (Figure 3), we also noted a more pronounced presence in the inner zone (Figure 5). Then, at stage II, the decrease in percent occupied area was greater for the inner zone than the rest of the flesh. Interpretation of those differences, however, requires further information regarding the timing of developmental patterns in the different fruit zones. Our results using image analysis of histological preparations concur with the acknowledged dilution pattern of SSCs within the pear flesh parenchyma matrix, and additionally provide further quantification and details of cellular differentiation and spatial differences within the fruit.

The microscope images (Figure 8) and the shape analysis (Table 2) of the fruit flesh parenchyma cells revealed pattern in which these cells lose roundness and become more irregular during expansive growth. This phenomenon has been previously described in pear fruits [14,19] as well in others such as olive [33], and could be precisely described using image analysis. In contrast to the irregularity in parenchyma cell shape, the stone cells maintain more rounded shapes due to the cessation of growth when their lignified secondary wall is first established in young and still rounded parenchyma cells, and the structural rigidity provided by further wall growth and lignification [19]. Furthermore, as stone cells initiated their formation early in fruit development, when the parenchyma cells from which they were differentiated were smaller and rounder, this timing undoubtedly influenced their geometry.

During fruit growth the shape of parenchyma cells whose cell walls are contiguous with the SCCs became notably more elongated than the rest of parenchyma cells, radiating outwards from around the SCCs. This event was previously described by Nii et al. [14], and appears to be a consequence of internal physical pressures during fruit expansion. That is, the lack of expansion by the lignified SSC cells restricts the possible directions for parenchyma cell growth within the fruit cell matrix. We also found that the parenchyma cells touching clusters are also larger than the other parenchyma cells at fruit maturity (Table 1). Larger parenchyma cells would likely indicate a lower presence of cell walls, suggesting softer fruit flesh immediately surrounding the SSCs, potentially producing a greater sense of disagreeable gritty texture to the fruit consumer.

4.4. Microscope image analysis techniques for advancing SCCs studies

Studying the SCCs in pear flesh presents some difficulties regarding how to best choose useful parameters to measure and evaluate characteristics such as their presence, formation, and distribution, among others. In general the evaluation of SCC content in pears has relied on separation techniques and the measurement of sclereid content weight, or by assessing the lignification process within the fruit [19,21,22,31,32,34–36]. While these methods have effectively revealed variation in SCC content among different varieties or in response to specific treatments or environmental factors, they offer limited insights into the developmental process of SCCs within the fruit. Conversely, studies utilizing microscope techniques have a relatively high cost-benefit ratio mainly due to the considerable time they require. These studies can be categorized into two groups: those that provide a descriptive view of SCC development [10,14,19,22,27,37] and those that employ histology for characterization, focusing solely on SCC content and size [15,17,20,23]. The quantitative measurements derived from microscopic analyses necessitate the acquisition of a large number of images, which are subsequently laboriously analyzed manually to obtain precise data. One promising solution to this challenge is the utilization of image-processing programs, which offer rapid, cost-effective, and highly precise image analysis. In our study, the implementation of these automatic programs has enabled the examination of a substantial number of images, ensuring the acquisition of precise information of a quantitative nature. Indeed, the use of image analysis helps form a bridge between anatomical observation and quantitative analytical techniques. This not only facilitates accurate confirmation or refutation of previously established knowledge, but also provides deeper insights into the development of SCCs within the pear flesh.

5. Conclusions

The RDI strategy examined in this study had no discernible impact on the quantity and size of stone cells in pear flesh. Consequently, it can be reasonably inferred that one of the fundamental goals of RDI strategies, which is to maintain fruit quality, has been successfully achieved. However, we emphasize the importance of considering the timing, intensity, and duration of water stress application during RDI strategies to avoid potential adverse effects on the textural quality of pears.

We employed automated image analysis programs, enabling us to conduct a more comprehensive analysis of the SCC characteristics in the fruit flesh. The study included examination of the quantity and size of stone cells within the SCCs, previously unfeasible using conventional tools. With these new data, we have not only been able to validate or refute existing knowledge with more accurate information derived from a substantial number of images and measurements, but have also acquired deeper insight regarding the development of pear fruit sclereids.

The authors believe that the information presented in this research can be used to develop more effective RDI strategies in pear cultivation to protect fruit quality, as well as to improve the understanding of SCC development in pear fruit flesh.

Author Contributions: Conceptualization, H.F.R.; methodology, H.F.R., D.P.L., A.C and J.D.P; software, A.C., D.P.L., and J.D.P.; investigation, H.F.R., D.P.L., A.C. and J.D.P.; resources, H.F.R., D.P.L. and A.C.; data curation, H.F.R., D.P.L. and A.C.; writing—original draft preparation, J.D.P.; writing—review and editing, H.F.R., D.P.L. and A.C; supervision, H.F.R., D.P.L. and A.C. ; funding acquisition, H.F.R., D.P.L. and A.C.

Funding: This research was supported by the Ministry of Universities of the Government of Spain (European Union–Next Generation funds) which financed the Grants for the Requalification of the Spanish University system of the University of Castilla–La Mancha.

Acknowledgments: The authors are grateful to Jordi Marsal and Joan Girona of IRTA, Institute of Agrifood Research and Technology, Barcelona, Spain, for providing fruits from the regulated deficit study which they performed [11].

Conflicts of Interest: The authors declare no conflict of interest.

References

1. Katerji, N.; Mastrorilli, M.; Rana, G. Water Use Efficiency of Crops Cultivated in the Mediterranean Region: Review and Analysis. *Eur J Agron* **2008**, *28*, 493–507, doi:10.1016/J.EJA.2007.12.003.
2. Chalmers, D.; Burge, G.; Jerie, P.H. and Mitchell, P.D. 1986, The Mechanism of Regulation of 'Bartlett' pear Fruit and Vegetative Growth by Irrigation Withholding and Regulated Deficit Irrigation. *J Am Soc Hortic Sci* **1986**, *111*(6), 904-907, doi: 10.21273/JASHS.111.6.904.
3. Galindo, A.; Collado-González, J.; Griñán, I.; Corell, M.; Centeno, A.; Martín-Palomo, M.J.; Girón, I.F.; Rodríguez, P.; Cruz, Z.N.; Memmi, H.; et al. Deficit Irrigation and Emerging Fruit Crops as a Strategy to Save Water in Mediterranean Semiarid Agrosystems. *Agric Water Manag* **2018**, *202*, 311–324, doi:10.1016/J.AGWAT.2017.08.015.
4. Mitchell, P.D.; Van Den Ende, B.; Jerie, P.H., Chalmers, D.J. Responses of 'Bartlett' pear to Withholding Irrigation, Regulated Deficit Irrigation, and Tree Spacing. *J Am Soc Hortic Sci* **1989**, *114*(1), 15-19, doi: 10.21273/JASHS.114.1.15
5. Vélez-Sánchez, J.E.; Balaguera-López, H.E.; Alvarez-Herrera, J.G. Effect of Regulated Deficit Irrigation (RDI) on the Production and Quality of Pear Triunfo de Viena Variety under Tropical Conditions. *Sci Hortic* **2021**, *278*, 109880, doi:10.1016/J.SCIENTA.2020.109880.
6. Caspari, H.W.; Behboudian, M.H.; Chalmers, D.J. Water Use, Growth, and Fruit Yield of 'Hosui' Asian Pears under Deficit Irrigation *J Am Soc Hortic Sci* **1994**, *119*, 383–388, doi:10.21273/JASHS.119.3.383.
7. Behboudian, M.H.; Lawes, G.S.; Griffiths, K.M. The Influence of Water Deficit on Water Relations, Photosynthesis and Fruit Growth in Asian Pear (*Pyrus Serotina* Rehd.). *Sci Hortic* **1994**, *60*, 89–99, doi:10.1016/0304-4238(94)90064-7.
8. Wu, Y.; Zhao, Z.; Wang, W.; Ma, Y.; Huang, X. Yield and Growth of Mature Pear Trees under Water Deficit during Slow Fruit Growth Stages in Sparse Planting Orchard. *Sci Hortic* **2013**, *164*, 189–195, doi:10.1016/J.SCIENTA.2013.09.025.
9. Wu, Y.; Zhao, Z.; Zhao, F.; Cheng, X.; Zhao, P.; Liu, S. Response of Pear Trees' (*Pyrus Bretschneideri* 'Sinkiangensis') Fine Roots to a Soil Water Regime of Regulated Deficit Irrigation. *Agronomy* **2021**, *11*, doi:10.3390/agronomy11112316.

10. Bain, J.M. Some Morphological, Anatomical, and Physiological Changes in the Pear Fruit (*Pyrus communis* Var. Williams Bon Chrétien) during Development and Following Harvest. *Aust J Bot* **1961**, 9, 99–123, doi:10.1071/BT9610099.
11. Marsal, J.; Rapoport, H.F.; Manrique, T.; Girona, J. Pear Fruit Growth under Regulated Deficit Irrigation in Container-Grown Trees. *Sci Hortic* **2000**, 85, 243–259, doi:10.1016/S0304-4238(99)00151-X.
12. Hsiao, T.C. Plant Responses to Water Stress. *Annu Rev Plant Physiol* **1973**, 24, 519–570, doi:10.1146/ANNUREV.PP.24.060173.002511.
13. Li, S.H.; Schneider, B.; Gershenzon, J. Microchemical Analysis of Laser-Microdissected Stone Cells of Norway Spruce by Cryogenic Nuclear Magnetic Resonance Spectroscopy. *Planta* **2007**, 225, 771–779, doi:10.1007/S00425-006-0376-Z/FIGURES/5.
14. Nii, N.; Kawahara, T.; Nakao, Y. The Development of Stone Cells in Japanese Pear Fruit. *J Hortic Sci Biotechnol* **2008**, 83, 148–153, doi: 10.1080/14620316.2008.11512362.
15. Cai, Y.; Li, G.; Nie, J.; Lin, Y.; Nie, F.; Zhang, J.; Xu, Y. Study of the Structure and Biosynthetic Pathway of Lignin in Stone Cells of Pear. *Sci Hortic* **2010**, 125, 374–379, doi:10.1016/J.SCIENTA.2010.04.029.
16. Cheng, X.; Cai, Y.; Zhang, J. Stone Cell Development in Pear. In: Korban, S. (eds) *The Pear Genome. Compendium of Plant Genomes*. Springer, Cham. **2019**, 201–225, doi:10.1007/978-3-030-11048-2_11.
17. Li, N.; Ma, Y.; Song, Y.; Tian, C.; Zhang, L.; Li, L. Anatomical Studies of Stone Cells in Fruits of Four Different Pear Cultivars. *Int J Agric Biol* **2017**, 19, 610–614, doi:10.17957/IJAB/15.0304.
18. Lee, S.H.; Choi, J.H.; Kim, W.S.; Han, T.H.; Park, Y.S.; Gemma, H. Effect of Soil Water Stress on the Development of Stone Cells in Pear (*Pyrus pyrifolia* Cv. 'Niitaka') Flesh. *Sci Hortic* **2006**, 110, 247–253, doi:10.1016/j.scienta.2006.07.012.
19. Choi, J.H.; Lee, S.H. Distribution of Stone Cell in Asian, Chinese, and European Pear Fruit and Its Morphological Changes. *J Appl Bot Food Qual* **2013**, 86, 185–189, doi:10.5073/JABFQ.2013.086.025.
20. Yan, C.; Yin, M.; Zhang, N.; Jin, Q.; Fang, Z.; Lin, Y.; Cai, Y. Stone Cell Distribution and Lignin Structure in Various Pear Varieties. *Sci Hortic* **2014**, 174, 142–150, doi:10.1016/J.SCIENTA.2014.05.018.
21. Wang, X.; Liu, S.; Liu, C.; Liu, Y.; Lu, X.; Du, G.; Lyu, D. Biochemical Characterization and Expression Analysis of Lignification in Two Pear (*Pyrus ussuriensis* Maxim.) Varieties with Contrasting Stone Cell Content. *Protoplasma* **2020**, 257, 261–274, doi:10.1007/S00709-019-01434-7/FIGURES/5.
22. Lee, S.H.; Choi, J.H.; Kim, W.S.; Han, T.H.; Park, Y.S.; Gemma, H. Effect of Soil Water Stress on the Development of Stone Cells in Pear (*Pyrus pyrifolia* Cv. 'Niitaka') Flesh. *Sci Hortic* **2006**, 110, 247–253, doi:10.1016/J.SCIENTA.2006.07.012.
23. Lee, S.-H.; Choi, J.-H.; Kim, W.-S.; Park, Y.-S.; Gemma, H. Effects of Calcium Chloride Spray on Peroxidase Activity and Stone Cell Development in Pear Fruit (*Pyrus pyrifolia* 'Niitaka'). *J Jpn Soc Hortic Sci* **2007**, 76(3), 191–196, doi: 10.2503/jjshs.76.191.
24. Gucci, R.; Lodolini, E.M.; Rapoport, H.F. Water Deficit-Induced Changes in Mesocarp Cellular Processes and the Relationship between Mesocarp and Endocarp during Olive Fruit Development. *Tree Physiol* **2009**, 29, 1575–1585, doi:10.1093/treephys/tpp086.
25. Johansen, D.A. *Plant Microtechnique*; McGraw-Hill Book Company: London, **1940**.
26. Ruzin, S.E. *Plant Microtechnique and Microscopy*; Oxford University Press: New York, **2000**; Vol. 198; ISBN 0195089561.
27. Sterling, C. Sclereid Development and the Texture of Barlett Pears. *J Food Sci* **1954**, 19, 433–443, doi:10.1111/J.1365-2621.1954.TB17474.X.
28. Pandey, V.P.; Singh, S.; Dwivedi, U. A Comprehensive Review on Function and Application of Plant Peroxidases. *Biochem Anal Biochem* **2017**, 6, doi:10.4172/2161-1009.1000308.
29. Torrecillas, A.; Corell, M.; Galindo, A.; Pérez-López, D.; Memmi, H.; Rodríguez, P.; Cruz, Z.N.; Centeno, A.; Intrigliolo, D.S.; Moriana, A. Agronomical Effects of Deficit Irrigation in Apricot, Peach, and Plum Trees. *Water Scarcity and Sustainable Agriculture in Semiarid Environment: Tools, Strategies, and Challenges for Woody Crops* **2018**, 87–109, doi:10.1016/B978-0-12-813164-0.00005-3.
30. Esau, K. *Anatomy of Seed Plants*; John Wiley & Sons: New York, **1898**.
31. Tao, S.; Khanizadeh, S.; Zhang, H.; Zhang, S. Anatomy, Ultrastructure and Lignin Distribution of Stone Cells in Two *Pyrus* Species. *Plant Sci* **2009**, 176, 413–419, doi:10.1016/J.PLANTSCI.2008.12.011.
32. Xue, C.; Yao, J.L.; Qin, M.F.; Zhang, M.Y.; Allan, A.C.; Wang, D.F.; Wu, J. PbrmIR397a Regulates Lignification during Stone Cell Development in Pear Fruit. *Plant Biotechnol J* **2019**, 17, 103–117, doi:10.1111/PBI.12950.
33. Rallo, P.; Rapoport, H.F. Early Growth and Development of the Olive Fruit Mesocarp. *J Hortic Sci Biotechnol* **2001**, 76, 408–412, doi:10.1080/14620316.2001.11511385.
34. Jin, Q.; Yan, C.; Qiu, J.; Zhang, N.; Lin, Y.; Cai, Y. Structural Characterization and Deposition of Stone Cell Lignin in Dangshan Su Pear. *Sci Hortic* **2013**, 155, 123–130, doi:10.1016/J.SCIENTA.2013.03.020.

35. Gong, X.; Xie, Z.; Qi, K.; Zhao, L.; Yuan, Y.; Xu, J.; Rui, W.; Shiratake, K.; Bao, J.; Khanizadeh, S.; et al. PbMC1a/1b Regulates Lignification during Stone Cell Development in Pear (*Pyrus bretschneideri*) Fruit. *Hortic Res* **2020**, *7*, doi:10.1038/s41438-020-0280-x.
36. Wang, X.; Liu, S.; Sun, H.; Liu, C.; Li, X.; Liu, Y.; Deguo Lyu; Du, G. Production of Reactive Oxygen Species by PuRBOHF Is Critical for Stone Cell Development in Pear Fruit. *Hortic Res* **2021**, *8*, 249, doi:10.1038/S41438-021-00674-0/42042642/41438_2021_ARTICLE_674.PDF.
37. Zhao, S. New Discoveries of Stone Cell Differentiation in Fruitlets of “Yali” Pears (*Pyrus bretschneideri* Rehd.). *J Food Agric Enviro* **2005**, *11*, 937-942, doi: 10.1234/4.2013.4776.

Disclaimer/Publisher’s Note: The statements, opinions and data contained in all publications are solely those of the individual author(s) and contributor(s) and not of MDPI and/or the editor(s). MDPI and/or the editor(s) disclaim responsibility for any injury to people or property resulting from any ideas, methods, instructions or products referred to in the content.